IEEE Access
Multidisciplinary | Rapid Review | Open Access Journal

Received June 23, 2020, accepted July 4, 2020, date of publication July 7, 2020, date of current version July 28, 2020.

Digital Object Identifier 10.1109/ACCESS.2020.3007848

NARX Prediction-Based Parameters Online Tuning Method of Intelligent PID System

JINGWEI LIU[1,2], TIANYUE LI[1], ZHEYU ZHANG[1], AND JIAMING CHEN[2]
[1]Information College, Capital University of Economics and Business, Beijing 100070, China
[2]Faculty of Information Technology, Beijing University of Technology, Beijing 100124, China

Corresponding author: Jingwei Liu (liujingwei@cueb.edu.cn)

ABSTRACT Control parameters of classical control system are expected to be online tuned and optimized by intelligent methods, in order to improve performance and help engineers reduce a lot of repetitive work in dangerous and harmful working environments. **Main ideas and works of this paper are as follows:**Firstly, change ratio based expert PID control method (EA-PID) is proposed to expand range of control parameters. Expert rule table (ERT) of expert PID control method (E-PID) is replaced by change ratio table (CRT) of EA-PID. Adjusted parameters of EA-PID are the results of multiplying change ratios in current adjusting cycle and control parameters in previous adjusting cycle. Secondly, NARX prediction-based NARX-E-PID and NARX-EA-PID are proposed. The NARX neural network is designed as a time series predictor to predict the output of the control system, then control parameters are adjusted according to the predicted output. Thirdly, comparative simulations of all the above methods are implemented to verify the improved effects. Finally, theoretical analysis is provided to ensure the stability of control systems. **Effect are as follows:** Firstly, comparative simulations verify that the improved methods have faster control speed, smaller steady-state error, less overshoot, and better ability of anti-interference. Secondly, theoretical analysis shows that the unstable control systems with adjusted parameters can be changed into a stable system by stability judgment in each adjusting cycle.

INDEX TERMS Control parameters online tuning, intelligent control, Expert-PID, NARX neural network, predictive control.

I. INTRODUCTION

Classical control is widely applied in industrial practices, which mostly relies on forms of closed loop control [1]. 90% of controllers in applications are PID controllers [2], [3] because classical PID control method has many advantages such as low cost, proved stability, and easy operation [4]. In order to make the PID control system have better performance, the parameters of controllers are expected to be online tuned and optimized [5].

There are several existing advanced control methods.

1) Adaptive control (ADC). Adaptive control can continuously identify model parameters and adjust control parameters to adapt the changes of the work environment [6]. Adaptive control has been proved that it can design stable, safe and automatic systems since it was birth in the last century. There are two types of existing adaptive PID control methods: direct and indirect adaptive PID control [7]. Direct adaptive control corrects PID controller coefficients based on the analysis of the controlled variable. Indirect adaptive control is based on controlled object model identification, and PID controller coefficients are corrected according to the result of this model. In adaptive control, obtaining a general model in theory is difficult. The process of parameter estimation takes a long time to converge. Therefore, the adjustments of parameters are more difficult than classical control.

2) Predictive control (PDC). Predictive control is based on a certain model. PDC uses the past input and output to predict the output in a certain period of time in the future. Then, it minimizes the result of quadratic objective function with control constraints and prediction errors, the optimal control law of the current and future cycle is obtained. Predictive control has strong robustness, and it has been widely used in industry since 1970s. It mostly aims at linear systems and helping engineers to build dynamic closed-loop system with good stability in a limited period of time [8]. The predictive control is insufficient for nonlinear systems and stochastic uncertain systems. It requires accurate models and high computing performance [9].

3) Gain scheduling control (GSC). Gain scheduling control can solve nonlinear problems because the gain scheduling controller is formed by interpolating between a set of

The associate editor coordinating the review of this manuscript and approving it for publication was Xiaochun Cheng.

linear controllers. The resulting controller is a linear system whose parameters are adjusted as a function of the exogenous scheduling variables. The control parameters are zoomed in or out according to the gain scheduling controller in each control cycle. Gain scheduling control is a simple extension of linear design, and it is mature in industrial applications. In gain scheduling control, the stability and performance need to be further verified from extensive simulation studies.

4) Artificial intelligent control (AIC). In AIC systems, the control variable is the output of AI controller and the input of controlled object, which is directly calculated by AI methods. The typical AIC methods include expert control, fuzzy control and neural network control. AIC methods have strong fault tolerance [10]. It can be used in nonlinear and complex control. In AIC control, models are complex and nonlinear, which make them difficult to be analyzed theoretically.

5) Artificial intelligence based improved classical control method (AI-CC). In AI-CC systems, AI is an intelligent module to adjust the parameters of classical controller. Take PID control for example, the input of AI module is same as the input of PID controller, and the outputs of AI module are the adjusted K_p, K_i, K_d. Comparing with AIC control, the adjusted objects of AI-CC are the parameters of controller. AI-CC has its own advantages: 1) Many practical applications are classical control especially PID control. AI-CC methods are much simpler and more feasible to improve and upgrade the existing classical control systems. 2) There are already mature theories of classic control, which can be used to analyze the AI-CC systems. 3) Various AI-CC methods can be implemented easily because these methods have little dependence between AI module and CC module. The output of AI module is the input of CC module. Therefore, AI-CC is the focus of this study. The problems of AI-CC methods are same as classical control because AI-CC methods are based on classical control.

Conclusion of the above research: Advantages of ADC, PDC, GSC, and AIC are considered in this study. Adaptive structure, change ratio, predictor, and intelligent methods are adopted and applied theoretically to the proposed AI-CC methods.

The motivations of this study are as follows: 1) Better performance are expected to be improved, such as faster control speed, smaller steady-state error, and better ability of anti-interference. 2) Stabilities of the improved methods are expected to be proven in theory. 3) Online tuning AI-CC methods are expected to reduce the repetitive, unhealthy and unsafe work of engineers in some applications.

A. RELATED WORK

The existing AI-CC methods include expert system based PID control (E-PID), fuzzy calculation based PID control (F-PID), neural network based PID control (NN-PID), and other artificial intelligent based PID control technologies, for example, genetic algorithm PID control [11]. F-PID can adjust control parameters online by fuzzy calculation, which is based on fuzzy rules and system statues such as the error between the output and input of control system. Fuzzy rules are designed according to the manual control rules [12]. Ji applied F-PID to robot arm motion control [13]. Dong used F-PID to realize the depth control for ROV in nuclear power plant [14]. NN-PID realizes parameters online tuning by training the weights of the neural network [15]. The target of training is to minimize the result of loss function. Typical NN-PID includes BPNN-PID and RBFNN-PID.

E-PID is a typical AI-CC method based on expert system, and it is similar to GSC. E-PID uses the expert system to adjust control parameters of classical PID control. E-PID is used in many applications because of its simple structure and mature theories [16]. Kang and Liang [17] applied E-PID to servo system, and the experimental result shows that E-PID can obtain excellent control effect. Luo and Li [18] applied E-PID to blood glucose control and obtained helpful results in medical [19]. In each adjustment cycle of E-PID, the control parameters are adjusted according to the expert rules tables (ERT) [20]. The differences between E-PID and GSC are as follows: 1) The inputs of ERT are the system error and the differential calculation result of the system error. The inputs of GSC are diverse, which are not only include the system error. 2) The ERT is designed according to expert experience, which is simple than the gain controller nonlinear model of GSC. The ERT of E-PID model is similar to the gain controller of GSC model. The gain controller of GSC model can solve the nonlinear problem of the linear PID control system. 3) The possible output values of adjusted results of E-PID are limited because the possible output values of ERT are limited. In this study, two improved methods based on E-PID are proposed.

Problems of the existing E-PID are as follows: 1) The reasoning process is based on the fixed rules or strict formulas. The control parameters are required to be configured specifically and accurately by manual based work before the system goes online. If the rules and formulas are incorrect, control parameters will not be tuned and optimized by the control system itself. 2) The adjustments of parameters are based on current system error, which leads the control speed of E-PID is fast but overshoot often occurs. 3) Stability of E-PID need to be guaranteed by theoretical analysis methods.

In order to solve the above problems, the advantages of ADC, PDC, GSC, and AIC are adopted into AI-CC. NARX (Nonlinear autoregressive with exogenous inputs Neural network) is a time series prediction method which can be adopted to predict the output of control system. NARX is the simplest type of recurrent neural network [21], which is faster than LSTM. In this study, NARX is adopted as the predictor to predict the system output at future time, then the control parameters are adjusted according to the predicted results in each cycle.

B. CONTRIBUTIONS

Main contributions of this study are as follows:

1) In order to improve the control performance, EA-PID method is proposed. The existing E-PID uses fixed

rules to adjust PID parameters, while EA-PID uses the change ratios to adjust tuning rules and PID parameters. The adjusted parameters of EA-PID are the multiplied results of change ratio and parameters in the last adjustment cycle. As a result, EA-PID has more flexible rules for tuning work and the performance of control system are improved.

2) In order to further improve the control performance, NARX-E-PID is proposed to maintain control speed and NARX-EA-PID is proposed to do better in overshoot suppressing. E-PID and EA-PID adjust control parameters only consider the current system output. However, for NARX-E-PID and NARX-EA-PID, the output of control system is predicted firstly by NARX predictor. Then, the control parameters are adjusted according to the predicted output. As a result, the ability of anti-interference is improved by both NARX-E-PID and NARX-EA-PID.
3) In order to verify the feasibility and the improvements of performance, unsaturated experiment (with short-term interference) and saturated experiment (with long-term interference) are implemented. Results of simulation show that the proposed methods are convergent, the performance are improved, and the ability of anti-interference are acceptable.
4) In order to verify the stability, theoretical analysis is implemented. Based on limitations and assumptions of classical control theories, the theoretical method of stability judgment is provided. A demo of unstable EA-PID control system is transformed into stable EA-PID-S system according to the proposed stability judgment method.

The rest of the paper is organized as follows: In **Section II**, existing classical PID and E-PID models are defined, the structure and flowchart for implementation are provided. In **Section III**, EA-PID model is proposed, and the improvements of EA-PID are described in detail. In **Section IV**, NARX-E-PID and NARX-EA-PID models are proposed, and the design of NARX predictor is described. In **Section V**, comparative simulations are implemented and the results of unsaturated simulation and saturated simulation are shown. In **Section VI**, stabilities of all the above models are theoretically analyzed. In **Section VII**, conclusions about advantages and disadvantages of all the methods are discussed, and future work is listed.

II. PID AND E-PID MODEL (EXISTING MODEL)

Section II is organized as follows: In part A, the existing PID model is described in detail. In part B, the existing Expert PID model is described in detail. Section II is the basis of the proposed methods and the following sections.

A. PID MODEL (EXISTING METHOD)

The structure of classical PID control model is shown in Fig.1. K_p is Proportional parameters P. K_i is integral parameters I. K_d is derivative parameters D. Each parameter is

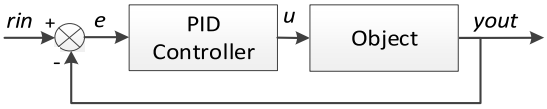

FIGURE 1. Structure of classical PID control systems.

independent of others. K_p, K_i, and K_d occur in separate terms of the controller and can produce a combined effect by adding them up. In classical PID control, the control parameters K_p, K_i, and K_d have been set as fixed values before the system starts.

In each control process at time t, the input of controlled object is the control variable u, which is the output of the PID controller. According to u, the output of controlled object is generated [22]. The control variable u is calculated by the PID controller according to the system error e. At each time t, $e(t)$ and $ec(t)$ are calculated based on system input and output. $ec(t)$ is the differential of $e(t)$, which can be expressed as de/dt.

The calculation formula of PID controller module can be expressed as (1):

$$u(t) = K_p \cdot (e(t) + \frac{1}{K_i}\int e(t)\,\mathrm{d}t + K_d\frac{\mathrm{d}e(t)}{\mathrm{d}t}) \tag{1}$$

The model of AI-CC controller can be defined as (2):

$$u(t) = K_p(t) \cdot (e(t) + \frac{1}{K_i(t)}\int e(t)\mathrm{d}t + K_d(t)\frac{\mathrm{d}e(t)}{\mathrm{d}t}) \tag{2}$$

At time $\boldsymbol{t}$, the output of controller is $\boldsymbol{u(t)} = \boldsymbol{u}(\boldsymbol{t}-\boldsymbol{1}) + \Delta\boldsymbol{u(t)}$. The adjusted $\boldsymbol{u(t)}$ is calculated according to the incremental PID method, which is expressed as (3):

$$\begin{aligned}\boldsymbol{\Delta}u(t) = {} & k_p(t)\,(e(t) - e\,(t-1)) + k_i(t)e(t) \\ & + k_d(t)\,(e(t) - 2e\,(t-1) + e\,(t-2))\end{aligned} \tag{3}$$

The output of control system is $y_{out}(t)$, which can be calculated according to the digital PID method for discrete systems. $r_{in}(t)$ is the input of the control system. The transfer function of the controlled object is discretized to $a\,(i)$ and $b\,(j)$, then $y_{out}(t)$ is calculated as (4) and the system error and is calculated as (5)

$$\begin{aligned}y_{out}(t) = {} & -a\,(2)\,y_{out}\,(t-1) - a\,(3)\,y_{out}\,(t-2) \\ & - a\,(4)\,y_{out}\,(t-3) + b\,(2)\,u\,(t-1) \\ & + b\,(3)\,u\,(t-2) + b\,(4)\,u\,(t-3)\end{aligned} \tag{4}$$

$$e(t) = y_{out}(t) - r_{in}(t) \tag{5}$$

According to the above calculation process and formulas of PID model, the pseudocode is provided as Algorithm 1.

B. E-PID MODEL (EXISTING METHOD)

Definition 1 (Adjustment Cycle (AC)): 1 AC is a control process at a fixed simulation time (e.g. $t = 3$). In each AC, the control parameters $kp(t)$, $ki(t)$, and $kd(t)$ are adjusted once according to system error $e(t)$and the differential $ec(t)$, then the control variable $u(t)$ will be calculated and system output $y_{out}(t)$ will be obtained.

Algorithm 1 The Existing Classical PID Method

1. Begin
2. Initialize PID control system;
3. While ($t \leq max\_t$) do:
4. Simulation time updated: $t = t + 1$;
5. System input$r_{in}(t)$ is updated;
6. Calculate $u(t)$ and $\Delta u(t)$ according to (5)(1) and (3);
7. Calculate $y_{out}(t)$ according to (4);
8. Calculate $e(t)$ according to (5);
9. End while
10. End

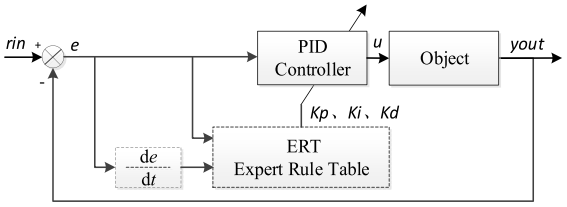

FIGURE 2. Structure of E-PID system.

Definition 2: (Expert-PID (E-PID)): E-PID is an intelligent PID control method based on classical PID. The parameters are online tuned by expert system in each AC.

The structure of E-PID control model is shown in Fig.2. E-PID combines the expert experiences with classical PID method. Different from classical PID method, the control parameters K_p, K_i, and K_d of E-PID will be adjusted in each AC according to expert rule table (ERT) [23], [6].

$e(t) = y_{out}(t) - r_{in}(t)$ is the error between of output of control and the input (target) of control system, and $ec(t) = \frac{de}{dt}$ is the differential of $e(t)$.

In E-PID method, the adjusted $K_p(t)$, $K_i(t)$, and $K_d(t)$ are queried directly from the expert rules table (ERT), which can be expressed as(6) to (8).

$$K_p(t) = R^E_{K_p}(e(t), ec(t)) \tag{6}$$

$$K_i(t) = R^E_{K_i}(e(t), ec(t)) \tag{7}$$

$$K_d(t) = R^E_{K_d}(e(t), ec(t)) \tag{8}$$

According to $e(t)$ and $ec(t)$, $K_p(t)$, $K_i(t)$, and $K_d(t)$ can be obtained directly from the E-PID rule table. In this study, the ERT is designed as TABLE 1.

Values in ERT are calculated by classical configuration method of PID system such as Z-N method [24] and Relay auto tuning method [25]. All the values are judged by stability criterion and the proposed AI-CC-S method in the following chapter.

The pseudocode of E-PID is shown as Algorithm 2.

III. EA-PID MODEL (PROPOSED METHOD 1)

Based on the existing E-PID in section II, section III is organized as follows: In Part A, idea of design and structure of EA-PID is proposed. In Part B, the change ratio table (CRT) of EA-PID is described in detail. In part C, the pseudocode of EA-PID is provided.

TABLE 1. Expert rules table.

(A) EXPERT RULE TABLE FOR PARAMETER K_p

$R^E_{K_p}(e(t), ec(t))$	$\|e\| \geq E_{high}$	$E_{low} \leq \|e\| < E_{high}$	$0 \leq \|e\| < E_{low}$
$\|ec\| \geq EC_{high}$	3	1.5	0.5
$EC_{low} \leq \|ec\| < EC_{high}$	3	1.5	0.5
$0 \leq \|ec\| < EC_{low}$	3	1.5	0.5

(B) EXPERT RULE TABLE FOR PARAMETER K_i

$R^E_{K_i}(e(t), ec(t))$	$\|e\| \geq E_{high}$	$E_{low} \leq \|e\| < E_{high}$	$0 \leq \|e\| < E_{low}$
$\|ec\| \geq EC_{high}$	0	0.000005	0.00001
$EC_{low} \leq \|ec\| < EC_{high}$	0	0.000005	0.00001
$0 \leq \|ec\| < EC_{low}$	0	0.000005	0.00001

(C) EXPERT RULE TABLE FOR PARAMETER K_d

$R^E_{K_d}(e(t), ec(t))$	$\|e\| \geq E_{high}$	$E_{low} \leq \|e\| < E_{high}$	$0 \leq \|e\| < E_{low}$
$\|ec\| \geq EC_{high}$	0	0.1	0.05
$EC_{low} \leq \|ec\| < EC_{hi}$	0	0.05	0.02
$0 \leq \|ec\| < EC_{low}$	0	0.01	0.01

Algorithm 2 The Existing E-PID Method

1. Begin
2. Initialize E-PID control system model;
3. Input Expert Rules' Table;
4. While ($\boldsymbol{t} \leq max\_t$) do:
5. Simulation time updated: $\boldsymbol{t = t + 1}$;
6. System input$\boldsymbol{r_{in}(t)}$is updated;
7. Calculate $\boldsymbol{e(t)}$ and $\boldsymbol{ec(t)}$;
8. Query $\boldsymbol{R^E_{Kp}}$, $\boldsymbol{R^E_{Ki}}$, $\boldsymbol{R^E_{Kd}}$ from ERT in TABLE 1;
9. $\boldsymbol{K_p(t)}$, $\boldsymbol{K_i(t)}$, $\boldsymbol{K_d(t)}$ are adjusted according to (6) to (8);
10. Calculate $\boldsymbol{u(t)}$ and $\boldsymbol{\Delta u(t)}$ according to (2) and (3);
11. Calculate $\boldsymbol{y_{out}(t)}$ according to (4);
12. End while
13. End

A. STRUCTURE OF EA-PID (PROPOSED METHOD 1)

In the existing E-PID, all the possible $K_p(t)$, $K_i(t)$, and $K_d(t)$ are set to limited values according to ERT. Hence, the performance and intelligent features of E-PID are limited. In order to solve this problem, EA-PID method is proposed in this study.

Definition 3: Change ratio based expert PID control method (EA-PID): In this study, EA-PID is an improved intelligent PID control method based on E-PID. Compared with E-PID, the ERT of E-PID is replaced by Change Ratio Table (CRT) in EA-PID. In EA-PID, the adjusted $K_p(t)$, $K_i(t)$, and $K_d(t)$ at time t are the multiplied result of change ratio $R_{Kp}(t)$, $R_{Ki}(t)$, and $R_{Kd}(t)$ at time t and $K_p(t-1)$, $K_i(t-1)$, $K_d(t-1)$ at time $t-1$, respectively.

The system structure of EA–PID method is provided in Fig.3. The outputs of multiplier are the adjusted $K_p(t)$, $K_i(t)$,

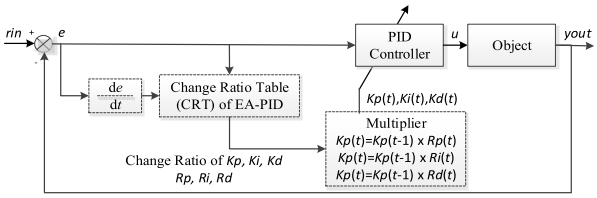

FIGURE 3. Structure of EA-PID.

TABLE 2. Change ratio table (CRT) of EA-PID.

(A) CRT FOR PARAMETER K_p

$R_{Kp}^{EA}(e(k), ec(k))$	$\|e\| \geq E_{high}$	$E_{low} \leq \|e\| < E_{high}$	$0 \leq \|e\| < E_{low}$
$\|ec\| \geq EC_{high}$	1	0.998	0.998
$EC_{low} \leq \|ec\| < EC_{high}$	1.002	1	1
$0 \leq \|ec\| < EC_{low}$	1.004	1.002	1

(B) CRT FOR PARAMETER K_i

$R_{Ki}^{EA}(e(k), ec(k))$	$\|e\| \geq E_{high}$	$E_{low} \leq \|e\| < E_{high}$	$0 \leq \|e\| < E_{low}$
$\|ec\| \geq EC_{high}$	1	0.998	0.998
$EC_{low} \leq \|ec\| < EC_{high}$	1.002	1	1
$0 \leq \|ec\| < EC_{low}$	1.004	1.002	1

(C) CRT FOR PARAMETER K_d

$R_{Kd}^{EA}(e(k), ec(k))$	$\|e\| \geq E_{high}$	$E_{low} \leq \|e\| < E_{high}$	$0 \leq \|e\| < E_{low}$
$\|ec\| \geq EC_{high}$	1.002	1.002	1.002
$EC_{low} \leq \|ec\| < EC_{high}$	1	1	1
$0 \leq \|ec\| < EC_{low}$	0.998	0.998	0.998

and $K_d(t)$. The inputs of the multiplier are change ratios and historical control parameters, i.e., $K_p(t-1)$, $K_i(t-1)$, and $K_d(t-1)$.

B. DESIGN OF CHANGE RATIO TABLE (CRT)

The Change Ratio Table (CRT) of EA-PID are designed as III-C according to expert experiences. The change ratios $R_{Kp}(t)$, $R_{Ki}(t)$, and $R_{Kd}(t)$ are proportions between the control parameters at time t and $t-1$, which can be expressed as $R_{kp}(t) = R_{Kp}^{EA}(e(t), ec(t))$. In each AC of EA-PID, the change ratio $R_{Kp}(t)$, $R_{Ki}(t)$, and $R_{Kd}(t)$ are queried firstly. Then, the value of the adjusted $K_p(t)$, $K_i(t)$, and $K_d(t)$ are calculated as (9) to (11):

$$K_p(t) = R_{K_p}^{EA}(e(t), ec(t)) \cdot Kp(t-1) \tag{9}$$

$$K_i(t) = R_{K_i}^{EA}(e(t), ec(t)) \cdot Ki(t-1) \tag{10}$$

$$K_d(t) = R_{K_d}^{EA}(e(t), ec(t)) \cdot Kd(t-1) \tag{11}$$

Change Ratio Table (CRT) of EA-PID method is provided in III-C, which is also designed according to the expert experiences. The maximum and minimum adjusted $K_p(t)$, $K_i(t)$, and $K_d(t)$ of EA-PID are around the scale of output values of ERT in TABLE 1.

CRT are designed based on the max and min values of ERT. The values of CRT are designed according to ERT to make the adjusted $K_p(t)$, $K_i(t)$, and $K_d(t)$ in a reasonable range. All the adjusted parameters of EA-PID will be verified by the proposed AI-CC-S method to make the control system stable.

Algorithm 3 EA-PID

```
Begin
Initialize EA-PID control system model;
Input Change Ratio Table (CRT);
While (t ≤ max_t) do:
    Simulation time updated: t = t + 1;
    System input r_in(t) is updated;
    Calculate e(t)and ec(t);
    Query R_Kp^EA, R_Ki^EA, R_Kd^EA from CRT in III-C;
    K_p(t), K_i(t), K_d(t) are adjusted by (9)-(11);
    Calculate u(t) and Δu(t) according to (2)-(3);
    Calculate y_out(t) according to (4);
End while
End
```

C. IMPLEMENT OF EA-PID

The pseudocode of EA-PID is designed as Algorithm 3.

IV. NARX-E-PID MODEL AND NARX-EA-PID MODEL (PROPOSED METHOD 2)

Based on the improved EA-PID method in section III, section IV is organized as follows: In part A, idea of NARX prediction-based AI-CC methods is proposed. In part B, the NARX based predictor is designed in detail. In part C, NARX-E-PID is described in detail. In part D, NARX-EA-PID is described in detail. In part E, the differences among E-PID, EA-PID, NARX-E-PID, and NARX-EA-PID are compared.

A. NARX PREDICTION-BASED AI-CC METHOD

The idea and principles for the improvement are as follows: In classical control, K_p, K_i, and K_d are fixed values which are adjusted before the system starts by engineers. The adjustments are on the basis of the control effects after each control process. For example, if the control results show that the control speed is slow, K_p should be adjusted larger. If the steady-state error is large, the K_i should be adjusted larger.

According to the above principle, new adjustments of K_p, K_i, and K_d will result in different effects. If the effects of adjustments can be predicted, the adjustments of K_p, K_i, K_d can be more accurate and effective. For example, if the predicted output of control system is far from the input (target value) which means the control speed is slow, then the online tuner will adjust K_p as a lager value to increase the control speed.

B. NARX PREDICTOR

1) STRUCTURE OF NARX PREDICTOR

NARX is a nonlinear autoregressive model which has exogenous inputs. It means that the model relates the current

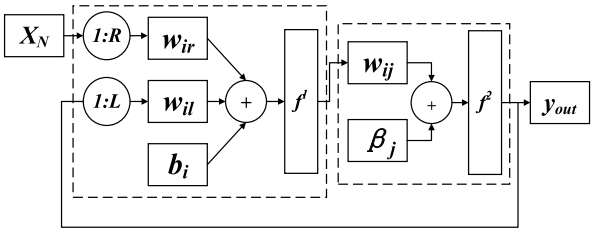

FIGURE 4. Structure of NARX.

TABLE 3. Meanings for symbols of NARX.

symbol	meaning
f	The activation function of hidden layer or output layer.
R	The time-delay order of input.
L	The time-delay order of output.
w_{ir}	The weight between the ith node of hidden layer and the rth time-delay node of input.
$x_{(t-r)}$	The current and delay values of input.
w_{il}	The weight between the ith node of hidden layer and the lth time-delay node of output.
$y_{(t-l)}$	The current and delay values of output.
b_i	The bias of the ith node of hidden layer.
w_{ij}	The weight between the ith node of hidden layer and the jth node of output layer.
β_j	The bias of the jth node of output layer.

value of a time series to both past values of the same series, current and past values of the exogenous series.

NARX model is a typical dynamic neural network. For the dynamic neural network, the output of network is fed back as the input to participate in the next training. Therefore, the network can remember the previous output.

In control system, the current output is related to the current input, the previous input, and the output. The NARX is a time series predictive method which can be adopted to predict the system output in the future time [26].

The structure of NARX model is shown in Fig.4.

The symbols are listed in TABLE 3.

The hyper-parameters of NARX (for training) include: number of hidden layers, time-delay order of input, and time-delay order of output [27], [28].

The number of hidden layers should not be set too large. The problems of too many hidden layers are as follows: Firstly, the calculated gradient of error in each adjustment cycle will be unstable, which also influence the convergence of the neural network. Secondly, the network will fall into a local minimum, which affects the precision of the model. Thirdly, the training time will be much longer. Therefore, the number of hidden layers is set as 1 in this study. In addition, time-delay order of input and time-delay order of output are set as 10, which means that the system input and output of previous 10 ACs are used to predict the current output.

2) CALCULATION OF NARX PREDICTOR

The input of NARX predictor at current time t are as follows: 1) system input $r_{in}(t)$, 2) control parameters ($K_p(t)$, $K_i(t)$, $K_d(t)$,) 3) control variable (output of controller) $u(t)$, and system output $y_{out}(t)$, which can be expressed as (12).

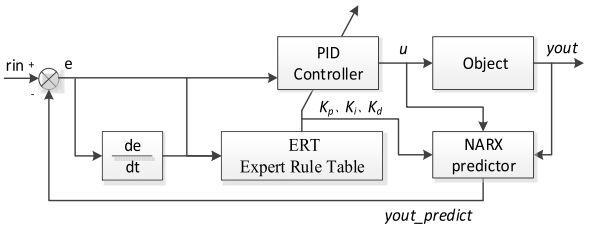

FIGURE 5. Structure of NARX-E-PID.

$$
\begin{aligned}
X_N &= \begin{Bmatrix} x_1\,(\text{t-R}) & \cdots & x_1\,(t-2) & x_1\,(t-1) \\ x_2\,(\text{t-R}) & \cdots & x_2\,(t-2) & x_2\,(t-1) \\ \vdots & \ddots & & \vdots \\ x_6\,(\text{t-L}) & \cdots & x_6\,(t-2) & x_6\,(t-1) \end{Bmatrix} \\
&= \begin{Bmatrix} r_{in}\,(\text{t-R}) & \cdots & r_{in}\,(t-2) & r_{in}\,(t-1) \\ K_p\,(\text{t-R}) & \cdots & K_p\,(t-2) & K_p\,(t-1) \\ K_i\,(\text{t-R}) & \cdots & K_i\,(t-2) & K_i\,(t-1) \\ K_d\,(\text{t-R}) & \cdots & K_d\,(t-2) & K_d\,(t-1) \\ u\,(\text{t-R}) & \cdots & u\,(t-2) & u\,(t-1) \\ y_{out}\,(\text{t-L}) & \cdots & y_{out}\,(t-2) & y_{out}\,(t-1) \end{Bmatrix} \\
&= \left\{ r_{inN}, K_{pN}, K_{iN}, K_{dN}, u_N, y_{outN} \right\} \qquad (12)
\end{aligned}
$$

In (12), $x_1\,(\text{t-r}), \cdots, x_1\,(t-2), x_1\,(t-1)$ is a one-dimensional ($D = 1$) vector time series from time $t - R$ to time $t - 1$. $X_1; X_2; \ldots, X_6$ is a six-dimensional vector time series ($D = 6$). In this study, $X_1; X_2; \ldots, X_6$ is composed of $r_{in}, K_p, K_i, K_d, u, y_{out}$ which is the input of NARX predictor.

The output of the ith node of hidden layer h_i can be expressed as (13).

$$h_i = tansig\left(\sum_{r=0}^{R} w_{ir} \cdot x_{(t-r)} + \sum_{l=0}^{L} w_{il} \cdot y_{(t-l)} + b_i\right) \qquad (13)$$

The output of the jth node of output layer $y_{out\_predict(t)}$ at future time t can be expressed as (14).

$$y_{out\_predict(t)} = purelin(\Sigma w_{ij} \cdot h_i + \beta_j) \qquad (14)$$

Before training, the weights of NARX are initialized randomly. During the training process, the weights of NARX are updated. The activation functions of the hidden layer, and the output layer are set as (15) and (16) respectively:

$$tansig\,(x) = \frac{2}{1 - e^{-2x}} - 1 \qquad (15)$$

$$purelin(x) = x \qquad (16)$$

C. NARX-E-PID MODEL (PROPOSED METHOD)

The structure of NARX-E–PID is shown in Fig.5. In NARX-E-PID model, NARX predictor is added to E-PID. The control parameters (K_p, K_i, K_d), system input r_{in}, control variable u, and system output y_{out} of past time (historical adjustment cycle) are used to predict system output $y_{out\_predict}$ at the future time t. In each AC, the value of system output y_{out} is replaced by the predicted output $y_{out\_predict}$. Then, the system error e and the differential of the system errorec can be calculated. Subsequently, the control parameters (K_p, K_i, and K_d) are adjusted by the E-PID method.

Algorithm 4 NARX-E-PID

1. Begin
2. Initialize the control system of NARX-E-PID;
3. Initialize inputDelays, feedbackDelays, hidden-LayerSize and trainFcn of NARX;
4. While ($t \leq max\_t$) do:
5. Simulation time updated: $t = t + 1$;
6. System input $r_{in}(t)$ is updated;
7. Calculate $u(t)$ and $\Delta u(t)$ according to (2) and (3);
8. Calculate $y_{out}(t)$ according to (4);
9. If predict begin==1 do:
10. Train *model* of NARX according to (13) and (14);
11. Calculate $y_{out\_predict(t)}$ according to NARX;
12. Calculate $e_{predict}\ (t+T)$and $ec_{predict}\ (t+T)$ according to $y_{out\_predict(t)}$;
13. Else
14. Calculate $e(t)$and $ec(t)$ according to $y_{out}(t)$;
15. End If
16. Train NN and update $W_{mn}(t)$ and $b_l(t)$;
17. Query $R^E_{Kp}, R^E_{Ki}, R^E_{Kd}$ according to ERT in TABLE 1;
18. Update parameters (online tuning) according to (6) to (8);
19. Calculate $u(t)$ and $\Delta u(t)$ according to (2) and (3);
20. Calculate $y_{out}(t)$ according to (4);
21. End while
22. End

Algorithm 5 NARX-EA-PID

1. Begin
2. Initialize the control system of NARX-EA-PID;
3. Initialize inputDelays, feedback Delays, hidden-LayerSize and trainFcn of NARX;
4. While ($t \leq max\_t$) do:
5. Simulation time updated: $t = t + 1$;
6. System input $r_{in}(t)$ is updated;
7. Calculate $u(t)$ and $\Delta u(t)$ according to (2) and (3);
8. Calculate $y_{out}(t)$ according to (4);
9. If predict begin==1 do:
10. Train *model* of NARX according to (13)-(14);
11. Calculate $y_{out\_predict(t)}$ according to NARX;
12. Calculate $e_{predict}\ (t+T)$ and $ec_{predict}\ (t+T)$ according to $y_{out\_predict(t)}$;
13. Else
14. Calculate $e(t)$and $ec(t)$ according to $y_{out}(t)$;
15. End If
16. Train NN and update $W_{mn}(t)$ and $b_l(t)$;
17. Query $R^{EA}_{Kp}, R^{EA}_{Ki}, R^{EA}_{Kd}$ according to CRT in III-C;
18. Update parameters (online tuning) according to (9) to (11);
19. Calculate $u(t)$ and $\Delta u(t)$ according to (2) and (3);
20. Calculate $y_{out}(t)$ according to (4);
19. End while
20. End

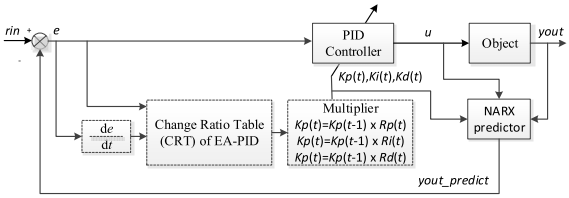

FIGURE 6. Structure of NARX-EA-PID.

According to the above NARX algorithm, the output of system at time $t+T$ can be predicted. t is the current time, and T is the order of the predictive steps. The input of NARX is the time series $\boldsymbol{X_N} = \{\boldsymbol{K_{pN}}, \boldsymbol{K_{iN}}, \boldsymbol{K_{dN}}, \boldsymbol{u_N}, \boldsymbol{y_{outN}}\}$ from time $\boldsymbol{t-N}$ to time $\boldsymbol{t-1}$. The output of NARX is $\boldsymbol{y_{predict}(t+T)}$. Then, the error $e_{predict}\ (t+T)$ at time $t+T$ can be calculated as IV-D. $r_{in}\ (t-1)$ is the input of the control system (target output of control system) at time $t-1$.

$$e_{predict}\ (t+T) = y_{out}\ (t+T) - r_{in}\ (t-1) \tag{17}$$

The pseudocode of the NARX-E-PID is presented as Algorithm 4.

D. NARX-EA-PID MODEL (PROPOSED METHOD)

NARX-EA-PID adds prediction to EA-PID. Similar to NARX-E-PID, NARX-EA-PID takes the NARX prediction as the first step to get $y_{out\_predict}$. After calculation, the control parameters are tuned by EA-PID. The structure of NARX-EA–PID method is shown in Fig.6.

The pseudocode of the NARX-EA-PID is presented as Algorithm 5.

E. COMPARISON AMONG E-PID, EA-PID, NARX-E-PID AND NARX-EA-PID

The differences among E-PID, EA-PID, NARX-E-PID, and NARX-EA-PID are listed in TABLE 4.

V. SIMULATION

All methods in section II, III, and IV are simulated in section V. Section V is organized as follows: In part A, the design of two types of simulations and unified configurations for all the existing and proposed methods are described. In part B, unsaturated simulations of E-PID, EA-PID, NARX-E-PID, and NARX-EA-PID methods are implemented in order to verify the effects of the improvements. In part C, saturated simulation is implemented in order to make sure that the output of control system of unsaturated simulation is unsaturated.

A. DESIGN OF SIMULATIONS

There are two types of experiments below:

1) **Unsaturated simulation.** The purpose of the unsaturated simulation is to verify the stability and the ability of anti-interference. The interference duration is set to 10 cycles, which is a very small value.
2) **Saturated simulation.** The purpose of the saturated simulation is to verify the convergence with long-term interference. It also verifies whether the short-term interference in the first experiment makes the system output saturated. The interference duration is set

TABLE 4. Comparison among E-PID, EA-PID, NARX-E-PID and NARX-EA-PID methods.

	E-PID	EA-PID	NARX-E-PID	NARX-EA-PID
Function of adjustment	new PID parameters are obtained directly from the rule table	new PID parameters at time t are calculated by old PID parameters at time $t-1$ with change ratio from the rule table	new PID parameters are obtained directly from the rule table	new PID parameters at time t are calculated by old PID parameters at time $t-1$ with change ratio from the rule table
Basis of adjustment	Expert Rule Table (ERT)	Change Ratio Table **(CRT)**	Expert Rule Table (ERT)	Change Ratio Table **(CRT)**
Output of ERT or CRT	PID parameters: $R^{E}_{K_p}(e(k), ec(k))$	**Change ratio**: $R^{EA}_{K_p}(e(k), ec(k))$	PID parameters: $R^{E}_{K_p}(e_{predict}(k), ec_{predict}(k))$	**Change ratio**: $R^{EA}_{K_p}(e_{predict}(k), ec_{predict}(k))$
Calculation of adjustment	$K_p(t) = R^{E}_{K_p}(t)$	$K_p(t) = K_p(t-1) \cdot R^{EA}_{K_p}(t)$	$K_p(t) = R^{E}_{K_p}(t)$	$K_p(t) = K_p(t-1) \cdot R^{EA}_{K_p}(t)$

as 2000, which is a big value. Problem of saturations can be solved with anti-windup structures.

Basic and unified configurations for all simulations: 1) In each AC, $\boldsymbol{K_p(t)}$, $\boldsymbol{K_i(t)}$, and $\boldsymbol{K_d(t)}$ parameters are adjusted only once. 2) Second-order control system with delay feature is assumed as a common controlled object model, which is modeled from a heater and expressed as $sys\,(s) = \frac{280}{s^2+25s+1} \cdot e^{-5s}$. The research scale is limited in common control system which controlled object can be considered approximately time-invariant. 3) Sampling period is set as $ts = 1$, which assumes that each AC costs 1 second. 4) The initial value of control parameters are set as $Kp\,(0) = 1, ki\,(0) = 0.0001$, and $Kd\,(0) = 0.1$, which are verified to be stable. 5) The input of control system is set as $rin(t) \equiv 1$ for step response.

B. UNSATURATED SIMULATION

Configuration for Unsaturated Experiment: 1) The max simulation time is set as $\max\_t = 2500$. 2) The start time of interference is $d\_t = 1500$. 3) The interference duration is set as $I\_t = 10$. 4) Interference intensity is set as $dst\_u(t) = 0.5$, which is added to the output of the PID controller. In summary, from simulation time 1500 to 1510, the control variable (output of PID controller) is changed to $u(t) + dst\_u(t)$.

Comparative simulation results of E-PID, EA-PID, NARX-E-PID, and NARX-EA-PID control systems are shown in Fig.7 respectively. The change curves of system input, system output, system error, control variable, and control parameters (K_p, K_i, and K_d) with simulation time are plotted. The horizontal axis of figures is the time t, the unit is seconds, and the vertical axis is the speed. The unit is radians / second.

In Fig.7, the change processes of control parameters, controller output, system output, and system error are shown. It is clear that all the above methods are convergent before and after the interference so the ability of anti-interference is acceptable.

According to the above simulations, the comparative charts and statistics results of system output of all the above 4 methods are drawn in Fig.8 and listed in TABLE 5.

TABLE 5 shows the performance of each method, and various evaluation indicators are compared. Data in the columns of rising time and settling time show features of control speed. Overshoot shows the ability of over-adjustment. Steady-state error shows the tracking ability of the control system. Data in the column of Max Deviation is the maximum difference between system output and input. Recovery time and Max Deviation shows the ability of anti-interference. Data in TABLE 5 are the mean value of ten experiments.

Fig.8 and TABLE 5 show that:

1) Performance of control speed: In this study, control speed is measured by Rising Time and Settling Time. The smaller Tr and Ts are, the better the performance of control speed is. NARX-E-PID is the fastest in 3 proposed methods (Rising Time is 67, Settling Time is 89). EA-PID (Rising Time is 165, Settling Time is 202) is faster than NARX-EA-PID (Rising Time is 167, Settling Time is 204). The rising curve (especially when AC is from 0 to 500) in Fig.8 shows that the control speed of NARX-E-PID is faster than EA-PID and NARX-EA-PID, and the speed of EA-PID is slightly faster than NARX-EA-PID.
2) Performance of steady-state error: Steady-state error is the deviation produced when the system changes from one steady state to another. Capability of output tracking input is measured by steady-state error. The steady-state error of EA-PID is the smallest among 4 methods (0.0021). The steady-state error of NARX-EA-PID (0.0040) is smaller than NARX-E-PID (0.0161). It can be seen that the curve of EA-PID is the closest to *rin* when AC is from 500 to 2000 in Fig.8.
3) Feature of overshoot: Data in the column of overshoot show the ability of over-adjustment. E-PID generated overshoot during the control process. All the proposed methods suppress overshoot, which means that the overshoot of 3 proposed methods are smaller than E-PID (0.1472). NARX-EA-PID has the smallest overshoot (0.0095) among the 3 proposed methods. The rising curve of E-PID exceeds the line of *rin* in Fig.8 when AC is from 0 to 500. However, the curves of all proposed methods are below the curve of E-PID. It means that the overshoot of E-PID is suppressed.

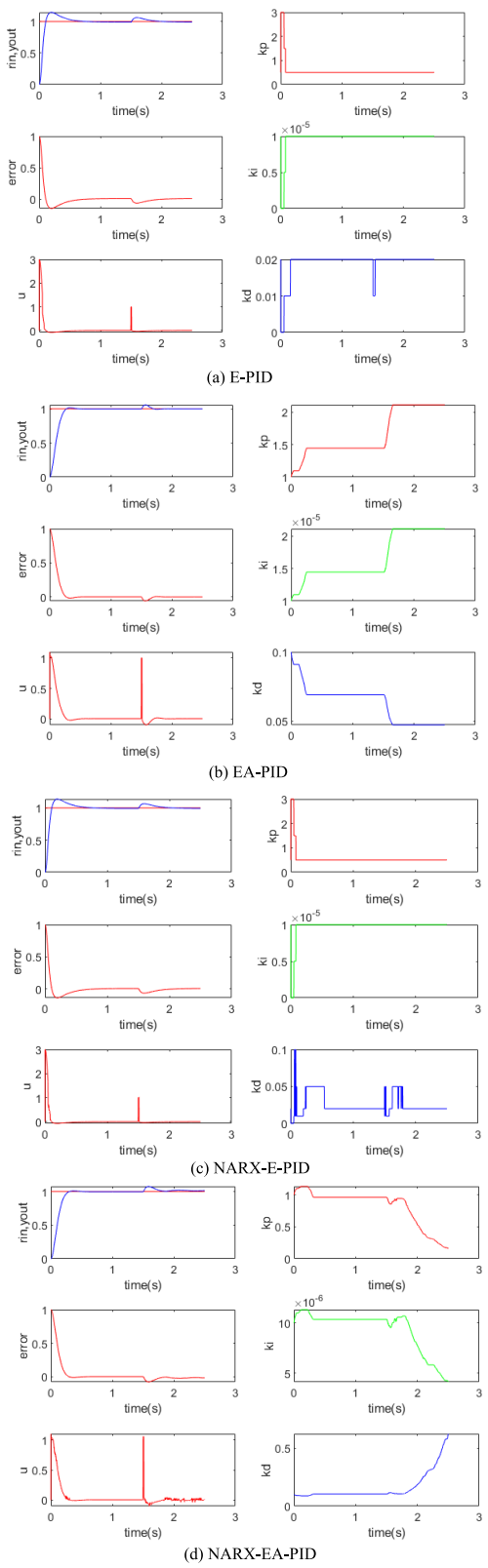

FIGURE 7. Comparative simulation results.

4) Ability of anti-interference: Data in the column of Max Deviation and recovery time show the ability of anti-interference. The Max Deviation of EA-PID is the smallest (1.0577) and the recovery time of EA-PID is the shortest (115), which proves the ability of anti-interference is the best. NARX-EA-PID (Recovery time is 207) is better than NARX-E-PID (Recovery time is 249). Recover curve (from AC is 1510) in Fig.8 shows that the recovery time of EA-PID is the shortest. NARX-EA-PID has the second good ability of anti-interference.

In summary, steady-state error and ability of anti-interference of EA-PID are the best among 4 methods. The performance reminded above of NARX-EA-PID is also improved compared with E-PID and NARX-E-PID. NARX-E-PID is the fastest among 3 proposed methods, and it also improve the ability of anti-interference. NARX-EA-PID is the best method in suppressing the overshoot.

C. SATURATED SIMULATION

Configuration for Saturated Experiment: 1) The max simulation time (max number of AC) is set as $\max\_t = 3500$ in order to ensure that the system can be stabilized and the interference can maximize the effect. 2) The start time of interference is at $d\_t = 1000$ (after the output reaches steady state). 3) The interference duration is set as $I\_t = 500$, in order to test the features of saturation and convergence of the system output. (4) Interference intensity (amplitude or strength of disturbance) is set as $dst\_u(t) = 0.5$, which is added to the output of the PID controller. In summary: From simulation time 2000 to 4000, the control variable is changed to $u(t) + dst\_u(t)$.

The system output curves in simulation results of the above 4 methods are shown in Fig.9.

According to Fig.9, the following conclusions can be drawn:

1) The system output y_{out} is unsaturated. The maximum values of system output in simulation 2 (Fig.9) prove that the control system is unsaturated in simulation 1 (Fig.8) because the amplitude of system output in simulation 2 (with longer time of interference) is larger than simulation 1.
2) All the proposed methods are convergent (stable) with long-term interference. The ability of long-term anti-interference of EA-PID, NARX-E-PID, and NARX-EA-PID are acceptable.
3) Comparative conclusions about performance among the above 4 methods according to Fig.9 are as follows: NARX-E-PID has the fastest control speed, but NARX-E-PID has bigger overshoot. EA-PID and NARX-EA-PID can suppress the overshoot. Compared with above 3 methods, the overshoot of NARX-EA-PID is the smallest. The steady-state error of EA-PID is the smallest before and after intervention. In addition, the Max Deviation of EA-PID is the smallest, and the recovery time of EA-PID is the shortest. EA-PID has the best ability of anti-interference. The results of unsaturated experiment (short-term

TABLE 5. Comparison of different intelligent control systems.

Comparison item→ Method↓	Rising Time	Settling Time	Steady-State Error	Overshoot	Max Deviation	Recovery time
E-PID	69(fast)	91(fast)	0.0088	0.1472	1.0636	345
EA-PID	165(slow)	202(slow)	**0.0021(smallest)**	**0.0153(improved)**	**1.0577(smallest)**	**115(fastest)**
NARX-E-PID	67(fastest)	89(fastest)	0.0161	0.1696	1.0639	**249(improved)**
NARX-EA-PID	167(slowest)	204(slowest)	**0.0040(improved)**	**0.0095(smallest)**	1.0698	**207(improved)**

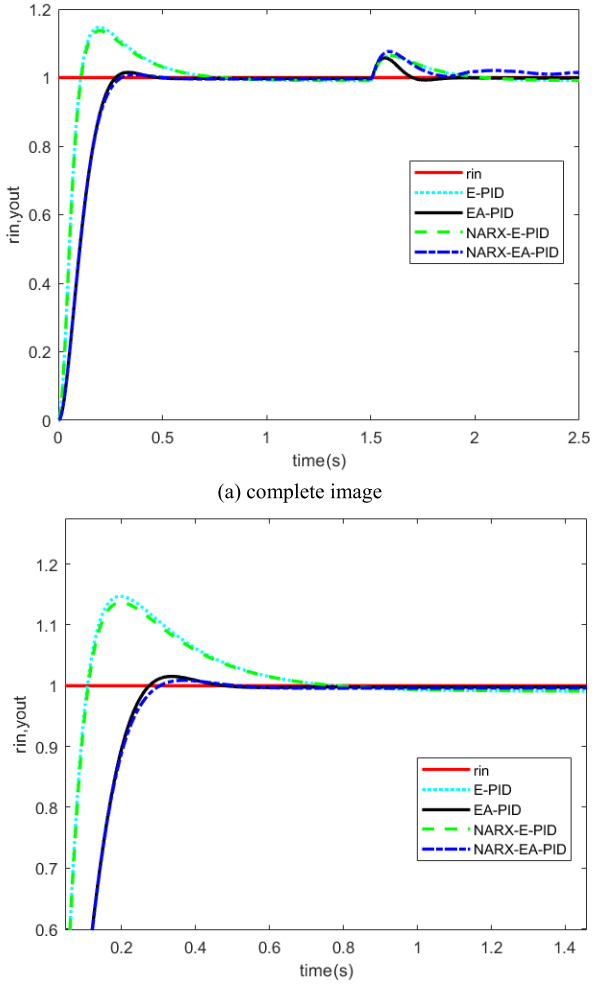

(a) complete image

(b) image details

FIGURE 8. Result of unsaturated experiment.

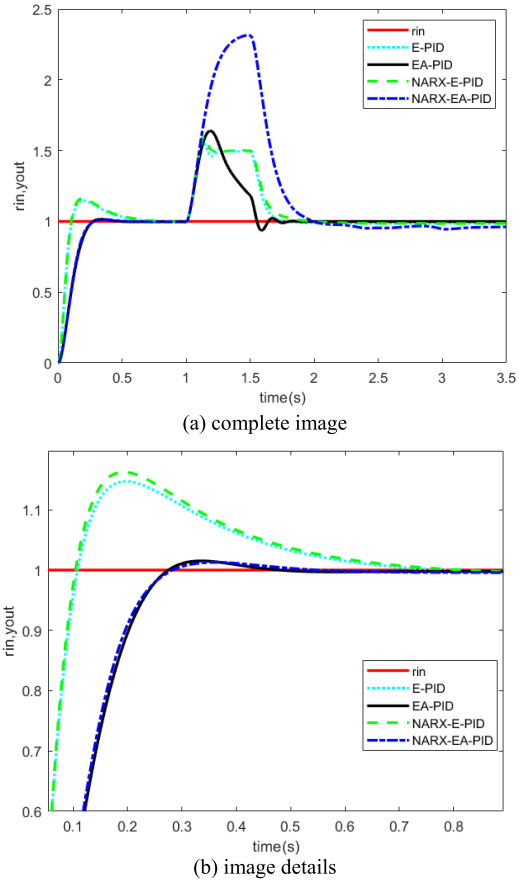

(a) complete image

(b) image details

FIGURE 9. Result of saturation experiment.

interference experiment) and saturated experiment (long-term interference experiment) are consistent.

VI. THEORETICAL ANALYSIS OF STABILITY

Stability of all the methods in section II, III, and IV are theoretically analyzed in section VI. Section VI is organized as follows: In part A, assumptions for analysis of stability are provided firstly. Then, the AI-CC models are converted to series of LTI models (defined as LTIs model) so classical analysis method of stability can be applied. In part B, theoretical analysis of stability is implemented, the stability judgment method for AI-CC system (defined as AI-CC-S method) are proposed. In part C, an example is provided to show how to judge stability of an AI-CC system in each AC. In part D, an example is provided to show how to improve an unstable EA-PID system to stable EA-PID-S system according to the above method.

A. ASSUMPTIONS AND LTIs MODEL

E-PID, EA-PID, NARX-E-PID, and NARX-EA-PID are based on classical PID so all the classical theories for PID control method can be used for system analysis such as features of stability, nonlinearity, etc.

Assumptions should be given first: 1) The research scope of controlled objects is limited to the common classical PID control applications. 2) In each AC (adjusting cycle), $K_p(t)$, $K_i(t)$, and $K_d(t)$ are fixed values, and the model of control system in each AC is classical PID control model with fixed control parameters. 3) The controlled object is time-invariant in each AC.

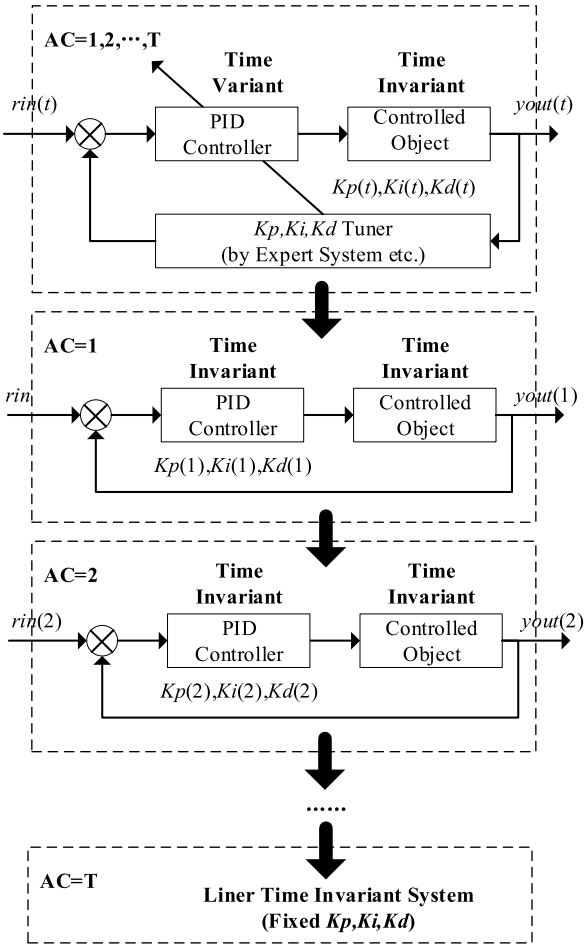

FIGURE 10. Converting from AI-CC systems to series of LTI systems.

With the above assumptions, the AI-CC system can be converted to series of LTI systems in each AC. The process of conversion is shown in Fig.10. Then, the classical analytical methods of PID system can be applied.

B. THEORETICAL ANALYSIS AND AI-CC-S MODEL

The open-loop transfer function of the AI-CC system is expressed as $G_{Open}(s) = G_{Ctr}(s) \cdot G_{Obj}(s)$, where $G_{Ctr}(s)$ represents the transfer function of the PID controller, and $G_{Obj}(s)$ represents the transfer function of controlled object. The closed-loop transfer function of the AI-CC system is expressed as $G_{Close}(s)$. All the above transfer functions can be expressed as (18) to (21):

$$G_{Ctr}(s) = K_p + K_i \cdot s + K_d \cdot \frac{1}{s} \tag{18}$$

$$G_{Obj}(s) = \frac{K}{\tau\sigma s^2 + (\tau + \sigma)s + 1} \cdot e^{-\tau s} \tag{19}$$

$$G_{Open}(s) = G_{Ctr}(s) \cdot G_{Obj}(s) \tag{20}$$

$$G_{Close}(s) = \frac{G_{Open}(s)}{1 + G_{Open}(s)} \tag{21}$$

Assume that $G_1(s) = e^{-ts}$ is the delay section, and $G_2(s) = \frac{M(s)}{N}$ is the system model. Therefore, the closed-loop system is $G_k(s) = \frac{M(s)\cdot e^{-ts}}{N(s)+M(s)\cdot e^{-ts}}$ and the frequency

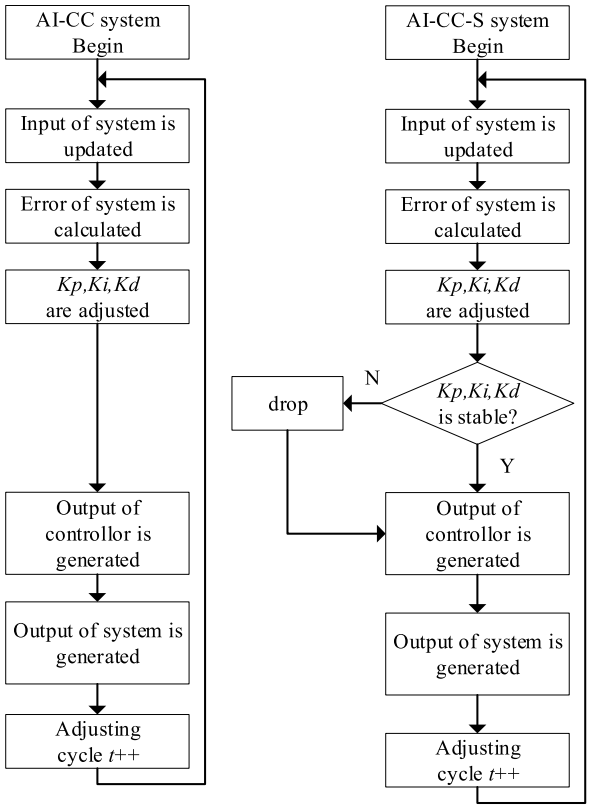

FIGURE 11. Difference between AI-CC and AI-CC-S methods.

characteristic of open loop system is $G_k(j\omega) = \frac{M(j\omega)}{N(j\omega)} \cdot e^{-j\omega t}$. If G2 is calculated as $G_2(j\omega) = A(\omega) \cdot e^{-j\theta(\omega)}$, G can beexpressed as $G(j\omega) = A(\omega) \cdot e^{-j[\theta(\omega)-\omega t]}$.

The Equivalent criterion of Nyquist stability criterion is:
When $L(\omega) = 0dB$, if $\varphi(\omega) > -\pi$, the system is stable.
When $\varphi(\omega) = -\pi$, if $L(\omega) < 0dB$, the system is stable.

Therefore, stability of AI-CC system can be judged by the following steps:

1) Only the stable parameters will be accepted in order to ensure the real-time stability of the system.
2) All unstable parameters will be rejected. In this case, the previous stable parameters are retained and used continuously.

Definition 3 (AI-CC-S Method): The AI-CC system is defined as AI-CC-S system, when all the adjusted $K_p(t)$, $K_i(t)$, $K_d(t)$ in each AC are judged according to the above two steps.

The difference between AI-CC system and AI-CC-S system can be found in Fig. 11.

Fig. 11 shows that, in each AC, adjusted $K_p(t)$, $K_i(t)$, and $K_d(t)$ are judged. Only stable parameters are accepted in each AC. If adjusted $K_p(t)$, $K_i(t)$, and $K_d(t)$ are unstable, $K_p(t-1)$, $K_i(t-1)$, and $K_d(t-1)$ are continued to be used.

C. EXAMPLE OF STABILITY JUDGMENT

The example of verification for the above theoretical stability analysis is provided as follows: In each AC,

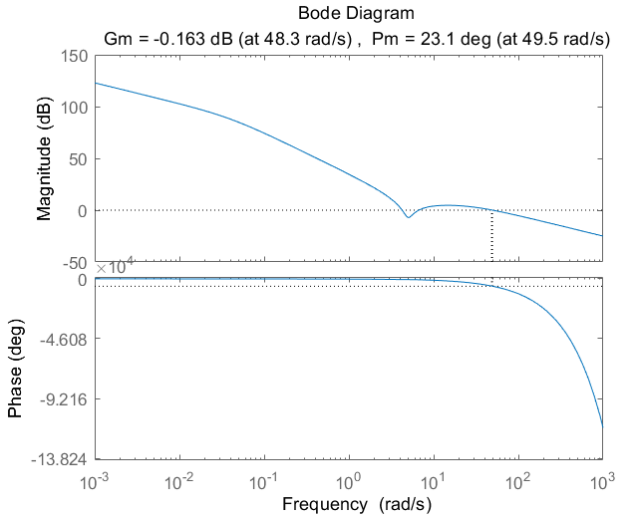

FIGURE 12. Bode plot result.

all adjusted control parameters are judged according to the above steps.

For example, if the controlled object model is $G_{Obj}(s) = \frac{280}{s^2+25s+1} + e^{-2s}$, the controller model is $G_{Ctr}(s) = k_p + \frac{k_i}{s} + k_d \cdot s = \frac{k_d \cdot s^2 + k_p \cdot s + k_i}{s}$, and the current time is t. The control parameters at time t are $K_p(t) = 0.2$, $K_i(t) = 0.2$ and $K_d(t) = 0.2$, which are pre-verified to stabilize the control system. Then, the open-loop transfer function $G_{Open}(s)$ can be calculated.

In each AC, amplitude margin and phase margin are calculated. The pseudocode is provided as follows, which can be implemented by different programming languages:

```
1. sys=tf(280,[1,25,1],'inputdelay',2);
2. sys_pid=tf([kd2bc,kp2bc,ki2bc],
   [1,0]);
3. sys_open=sys*sys_pid;
4. [bode_mag,bode_phase,bode_w]
   =bode(sys_open);
5. [bode_gm,bode_pm,bode_wcg,bode_wcp]
   =margin(bode_mag,bode_phase,bode_w);
```

The bode plots of control system with the latest $K_p(t)$, $K_i(t)$, and $K_d(t)$ are shown in Fig.10, which also contains the calculated results of amplitude margin and phase margin. The amplitude margin is calculated as $Gm = 20 \cdot log_{10}(gm) = -0.163dB < 0$, and the phase margin is calculated as $Pm = pm = 23.1\text{deg} > -\pi$. According to the above theoretical analysis, the current adjusted parameters $K_p(t)$, $K_i(t)$, and $K_d(t)$ can make the system work steadily, which means that the adjusted $K_p(t)$, $K_i(t)$, $K_d(t)$ can be adopted for PID controller.

D. EXAMPLE OF AI-CC-S METHOD

In order to verify AI-CC-S method which can change an unstable AI-CC system to a stable AI-CC-S system, unstable control parameters (unstable change ratio table) are designed firstly in TABLE 6.

TABLE 6. Change ratio table (CRT) for unstable EA-PID.

(A) CRT FOR PARAMETER K_p

$R_{Kp}^{EA}(e(k), ec(k))$	$\|e\| \geq E_{high}$	$E_{low} \leq \|e\| < E_{high}$	$0 \leq \|e\| < E_{low}$
$\|ec\| \geq EC_{high}$	1	0.92	0.92
$EC_{low} \leq \|ec\| < EC_{high}$	1.08	1	1
$0 \leq \|ec\| < EC_{low}$	1.16	1.08	1

(B) CRT FOR PARAMETER K_i

$R_{Ki}^{EA}(e(k), ec(k))$	$\|e\| \geq E_{high}$	$E_{low} \leq \|e\| < E_{high}$	$0 \leq \|e\| < E_{low}$
$\|ec\| \geq EC_{high}$	1	0.92	0.92
$EC_{low} \leq \|ec\| < EC_{high}$	1.08	1	1
$0 \leq \|ec\| < EC_{low}$	1.16	1.08	1

(C) CRT FOR PARAMETER K_d

$R_{Kd}^{EA}(e(k), ec(k))$	$\|e\| \geq E_{high}$	$E_{low} \leq \|e\| < E_{high}$	$0 \leq \|e\| < E_{low}$
$\|ec\| \geq EC_{high}$	1.08	1.08	1.08
$EC_{low} \leq \|ec\| < EC_{high}$	1	1	1
$0 \leq \|ec\| < EC_{low}$	0.92	0.92	0.92

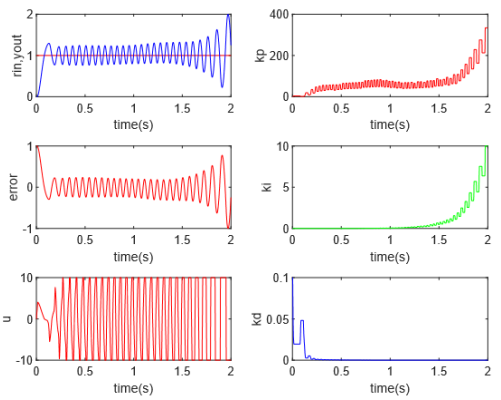

FIGURE 13. Simulation result of unstable AI-CC system.

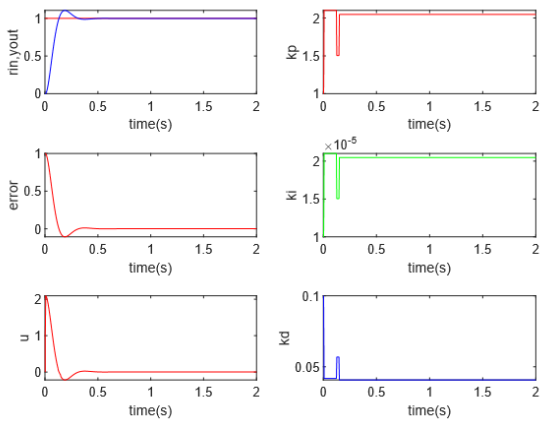

FIGURE 14. Simulation result of AI-CC-S system.

Except for the above CRT and max_t = 2000, all the other configurations of EA-PID simulation are set the same

TABLE 7. Comparison of different intelligent control systems.

Method→ Comparison Item↓	E-PID	EA-PID	NARX-E-PID	NARX-EA-PID
Stability (Convergence)	All stable 100% convergence	All stable 100% convergence	All stable 100% convergence	All stable 100% convergence
Control Speed (means of Tr and Ts)	**(69,91)**	(165,202)	**(67,89)**	(167,204)
Output tracking input capability (means of Steady-state error)	(0.0088)	**Best (0.0021)**	(0.0161)	**improved (0.0040)**
Anti-interference speed (means of recovery time)	(345)	**Best (115)**	**improved (249)**	**improved** (207)
Contents of configuration work for engineers	ERT for K_{pid}^{E}	CRT for R_{pid}^{EA}	ERT for K_{pid}^{E} and parameters of NARX predictor	CRT for R_{pid}^{EA} and parameters of NARX predictor
Accuracy requirements of configuration work (Estimation of workload)	Configuration of ERT needs to be very accurate (8 hours)	Configuration of CRT need not be accurate (2-4 hours)	Configuration of ERT needs to be accurate (4-8 hours)	Configuration of CRT need not be accurate (1-3 hours)

as configurations of unsaturated simulation in the previous chapter.

Firstly, EA-PID control process is simulated, the result of EA-S-PID simulation is shown in Fig 13. Fig.13 shows that the result of EA-PID system is unstable. The instability occurs because of CRT of TABLE 6.

Secondly, the EA-S-PID system is simulated, and the result of EA-S-PID simulation is shown in Fig.14. In EA-S-PID, all the unstable control parameters are denied. As a result, the result of EA-PID system is stable.

Comparing Fig 13 and Fig.14, the unstable result of EA-PID is change to stable result of EA-S-PID because all the adjusted parameters are judged to be stable.

VII. CONCLUSION

In this study, 3 AI-CC methods (EA-PID, NARX-E-PID, and NARX-EA-PID) are proposed. The adjust rules of control parameters of E-PID are replaced by the change ratio rules of EA-PID, and the updated parameters are calculated by multiplying the change ratio and the last control parameters. In NARX-E-PID and NARX-EA-PID, the predictor of NARX neural network are adopted to predict the system output in future so e and ec can be calculated. According to predictive e and ec, control parameters can be obtained in the rule table of E-PID and improved rule table of EA-PID respectively.

Comparative simulation results among E-PID, EA-PID, NARX-E-PID, and NARX-EA-PID methods can be summarized in TABLE 7. Contents of parameter configuration work and workload and operating time are estimated. Hence, the intelligent level of 4 methods and the ability requirements for engineers can be evaluated.

In TABLE 7, the first row lists the comparative methods, and the following rows show the stability, control speed, steady-state error, and ability of ante-interference. The last two rows show the contents and requirements of configuration work for engineers.

According to TABLE 7, conclusions can be summarized as follows:

1) The improvements of the EA-PID are as follows: EA-PID is a feasible and stable control method. The control speed of EA-PID is slightly faster than NARX-EA-PID. The steady-state error of EA-PID is smaller than E-PID, NARX-E-PID, and NARX-EA-PID. The recovery time of EA-PID is the shortest. It means that the ability of anti-interference of EA-PID is the best. Besides, EA-PID can suppress the overshoot. The overshoot of EA-PID is smaller than E-PID.
2) The improvements of the NARX-E-PID are as follows: NARX-E-PID method adds NARX prediction to E-PID method. NARX-E-PID is faster than E-PID and EA-PID. Rising Time and Settling Time of NARX-E-PID are smaller than them of E-PID. NARX-E-PID also improves the ability of anti-interference.
3) The improvements of the NARX-EA-PID are as follows: NARX-EA-PID is based on NARX prediction and improved Expert rule table. The steady-state error of NARX-EA-PID is smaller than E-PID and NARX-E-PID. The ability of overshoot suppressing of NARX-EA-PID is the best compared with other proposed methods. In addition, the recovery time is smaller than E-PID and NARX-E-PID, which means that it has good ability of anti-interference.
4) The conclusions of stability analysis of all the above proposed methods are as follows: All the methods are stable. In other words, all the methods have 100% convergence. The applications of them are accepted.
5) The configuration work of EA-PID and NARX-EA-PID is easier than E-PID and NARX-E-PID because the rules of control parameters can be optimized online. In addition, because NARX-E-PID and NARX-EA-PID are more intelligent than E-PID and NARX-E-PID, the workload of engineers is reduced. The configuration work required by engineers of EA-PID is less than E-PID, and the configuration work of NARX-EA-PID is less than NARX-E-PID.

In summary, the effects of EA-PID are improved as follows: the steady-state error is decreased; the overshoot is suppressed; the ability of anti-interference is improved. The improved effects of NARX-E-PID and NARX-EA-PID are that the ability of anti-interference is better than E-PID. The control speed of NARX-E-PID is faster than EA-PID. NARX-EA-PID has the best effect in suppressing the overshoot.

Future work may include: 1) More accurate predictive methods are expected to be adopted to improved AI-CC methods. 2) More AI-CC methods can be improved by adding NARX predictor such as F-PID and NN-PID. 3) More practical applications such as transportation, medical and industries will be verified by applying EA-PID, NARX-E-PID, and NARX-EA-PID.

REFERENCES

[1] J. Günther, E. Reichensdörfer, P. M. Pilarski, and K. Diepold, "Interpretable PID parameter tuning for control engineering using general dynamic neural networks: An extensive comparison," 2019, *arXiv:1905.13268*. [Online]. Available: http://arxiv.org/abs/1905.13268

[2] J. Fišer and P. Zítek, "PID controller tuning via dominant pole placement in comparison with ziegler-nichols tuning," *IFAC-PapersOnLine*, vol. 52, no. 18, pp. 43–48, 2019.

[3] Y. M. Zhao, W. F. Xie, and X. W. Tu, "Performance-based parameter tuning method of model-driven PID control systems," *ISA Trans.*, vol. 51, no. 3, pp. 393–399, May 2012.

[4] R.-E. Precup, S. Preitl, E. M. Petriu, J. K. Tar, M. L. Tomescu, and C. Pozna, "Generic two-degree-of-freedom linear and fuzzy controllers for integral processes," *J. Franklin Inst.*, vol. 346, no. 10, pp. 980–1003, Dec. 2009.

[5] M. Farahani, S. Ganjefar, and M. Alizadeh, "Intelligent control of SSSC via an online self-tuning PID to damp the subsynchronous oscillations," in *Proc. 20th Iranian Conf. Electr. Eng. (ICEE)*, May 2012, pp. 336–341.

[6] I. Carlucho, M. De Paula, S. A. Villar, and G. G. Acosta, "Incremental Q-learning strategy for adaptive PID control of mobile robots," *Expert Syst. Appl.*, vol. 80, pp. 183–199, Sep. 2017.

[7] A. G. Alexandrov and M. V. Palenov, "Adaptive PID controllers: State of the art and development prospects," *Autom. Remote Control*, vol. 75, no. 2, pp. 188–199, Feb. 2014.

[8] J. Richalet, "Industrial applications of model based predictive control," *Automatica*, vol. 29, no. 5, pp. 1251–1274, Sep. 1993.

[9] P. Cortes, M. P. Kazmierkowski, R. M. Kennel, D. E. Quevedo, and J. Rodriguez, "Predictive control in power electronics and drives," *IEEE Trans. Ind. Electron.*, vol. 55, no. 12, pp. 4312–4324, Dec. 2008.

[10] Y. Liao, L. Wang, Y. Li, Y. Li, and Q. Jiang, "The intelligent control system and experiments for an unmanned wave glider," *PLoS ONE*, vol. 11, no. 12, Dec. 2016, Art. no. e0168792.

[11] N. Pratama, F. X. Manggau, and P. Betaubun, "Attitude quadrotor control system with optimization of PID parameters based on fast genetic algorithm," *Int. J. Mech. Eng. Technol.*, vol. 10, no. 1, pp. 335–343, 2019.

[12] H. Khodadadi and H. Ghadiri, "Fuzzy logic self-tuning PID controller design for ball mill grinding circuits using an improved disturbance observer," *Mining, Metall. Explor.*, vol. 36, no. 6, pp. 1075–1090, Dec. 2019.

[13] Y. Ji, Y. Sun, and F. Wen, "Robot arm motion control based on trapezoidal fuzzy PID algorithm," in *BASIC & Clinical Pharmacology & Toxicology*, vol. 126. Hoboken, NJ, USA: Wiley, 2020, pp. 193–194.

[14] M. Dong, J. Li, and W. Chou, "Depth control of ROV in nuclear power plant based on fuzzy PID and dynamics compensation," *Microsyst. Technol.*, vol. 26, no. 3, pp. 811–821, Mar. 2020.

[15] O. A. Dahunsi, J. O. Pedro, and O. T. Nyandoro, "System identification and neural network based PID control of servo-hydraulic vehicle suspension system," *SAIEE Afr. Res. J.*, vol. 101, no. 3, pp. 93–105, Sep. 2010.

[16] Z. Jing, "Application and study of expert PID intelligent control," in *Proc. IOP Conf., Mater. Sci. Eng.*, vol. 563, no. 4. Bristol, U.K.: IOP Publishing, 2019, Art. no. 042084.

[17] F. Kang and Y. B. Liang, "Research on modeling and simulation of expert_PID controlled servo system based on matlab/s-function," in *Applied Mechanics and Materials*, vol. 347. Kapellweg, Switzerland: Trans Tech Publications, 2013, pp. 604–609. [Online]. Available: https://www.scientific.net/Home/Contacts

[18] Z. Luo and W. Li, "Tracking of mobile robot expert PID controller design and simulation," in *Proc. Int. Symp. Comput., Consum. Control*, Jun. 2014, pp. 566–568.

[19] Z. Z. Qian, G. C. Xin, and J. N. Tao, "Predictive control based on fuzzy expert PID tuning control," in *Advanced Materials Research*, vol. 466. Kirkland, QC, Canada: Electronics.ca Publications, 2012, pp. 1207–1211. [Online]. Available: https://www.electronics.ca/contact

[20] J. Xu, "An expert PID control algorithm based on anti-integration saturation," in *Proc. IEEE 2nd Adv. Inf. Technol., Electron. Autom. Control Conf. (IAEAC)*, Mar. 2017, pp. 1536–1539.

[21] G. Abbas, M. Nawaz, and F. Kamran, "Performance comparison of NARX & RNN-LSTM neural networks for LiFePO4 battery state of charge estimation," in *Proc. 16th Int. Bhurban Conf. Appl. Sci. Technol. (IBCAST)*, Jan. 2019, pp. 463–468.

[22] B. B. Jakovljević, T. B. Šekara, M. R. Rapaić, and Z. D. Jeličić, "On the distributed order PID controller," *AEU-Int. J. Electron. Commun.*, vol. 79, pp. 94–101, Sep. 2017.

[23] Q. X. Liu, "Design of flow control system based on expert PID," in *Proc. Int. Symp. Comput., Consum. Control (IS3C)*, Jul. 2016, pp. 1031–1034.

[24] C. C. Hang, K. J. Astrom, and Q. G. Wang, "Relay feedback auto-tuning of process controllers—A tutorial review," *J. Process Control*, vol. 12, no. 1, pp. 143–162, 2002.

[25] J. Berner, T. Hägglund, and K. J. Åström, "Asymmetric relay autotuning–Practical features for industrial use," *Control Eng. Pract.*, vol. 54, pp. 231–245, Sep. 2016.

[26] M. Zounemat-Kermani, D. Stephan, and R. Hinkelmann, "Multivariate NARX neural network in prediction gaseous emissions within the influent chamber of wastewater treatment plants," *Atmos. Pollut. Res.*, vol. 10, no. 6, pp. 1812–1822, Nov. 2019.

[27] S. M. Guzman, J. O. Paz, and M. L. M. Tagert, "The use of NARX neural networks to forecast daily groundwater levels," *Water Resour. Manage.*, vol. 31, no. 5, pp. 1591–1603, Mar. 2017.

[28] Z. Boussaada, O. Curea, A. Remaci, H. Camblong, and N. Mrabet Bellaaj, "A nonlinear autoregressive exogenous (NARX) neural network model for the prediction of the daily direct solar radiation," *Energies*, vol. 11, no. 3, p. 620, Mar. 2018.

JINGWEI LIU was born in Beijing, China, in 1982. He received the Ph.D. degree in control science and engineering (pattern recognition and intelligent system) from the Department of Electronic Information and Control Engineering, Beijing University of Technology, Beijing, in 2014.

Since 2014, he has been an Associate Professor with the Information College, Capital University of Economics and Business, where he served as the Director of the Software Research and Development Center, Information College. He has published three academic monographs, more than 20 academic articles, and holds 20 patents. His research interests include artificial intelligence, automatic control, intelligent control, and intelligent systems. He received the first prize of Teaching Achievements, the first prize of Teaching Basic Skills Competition, and the Most Popular Student Recognition Award.

TIANYUE LI was born in Hebei, China, in 1997. She received the B.S. degree from the Quality and Technical Supervision College, Hebei University, in 2019. She is currently pursuing the M.S. degree with the Management Engineering College, Capital University of Economics and Business. She is also a Research Member of the Big Data and Intelligent Transportation Research Center, Management Engineering College. Her research interests include artificial intelligence, deep learning, and intelligent control.

ZHEYU ZHANG was born in Hohhot, China, in 1998. He is currently pursuing the bachelor's degree in big data analysis with the School of Management Engineering, Capital University of Economics and Business.

From 2017 to 2020, he received the First-Class Scholarship twice, three software copyrights in Copyright administration of the People's Republic of China, participated in the preparation of monographs, and innovative training programs for college students. His research interests include machine learning and neural networks.

JIAMING CHEN was born in Beijing, China, in 1994. He received the M.S. degree in software engineering from the Capital Normal University, Beijing, China, in 2019. He is currently pursuing the Ph.D. degree in computer science with the Beijing University of Technology.

In 2018, he was a Researcher and an Assistant Tutor with the Big Data College, Huike Education Corporation. From 2016 to 2018, he was a Frontend Architect of Chengdu iDelta Technology Company Ltd. His research interests include artificial intelligence, brain–computer interface, and data mining. He received the Scholarship at Capital Normal University, from 2016 to 2018, and won the Third Prize in the Contest of Lan Qiao Cup, in 2017.